Chemosphere 283 (2021) 131196

Contents lists available at ScienceDirect

Chemosphere

journal homepage: www.elsevier.com/locate/chemosphere

Elucidating the bioremediation mechanism of *Scenedesmus* sp. IITRIND2 under cadmium stress

Shweta Tripathi [a], Neha Arora [a,1], Vikas Pruthi [a], Krishna Mohan Poluri [a,b,*]

[a] Department of Biotechnology, Indian Institute of Technology Roorkee, Roorkee, 247667, Uttarakhand, India
[b] Centre for Transportation Systems, Indian Institute of Technology Roorkee, Roorkee, 247667, Uttarakhand, India

ARTICLE INFO

Handling Editor: Chang-Ping Yu

Keywords:
Microalga
Scenedesmus sp.
Cadmium
Fatty acid methyl esters
Bioremediation

ABSTRACT

Cadmium (Cd) is a non-biodegradable pollutant that has become a global threat due to its bioaccumulation and biomagnification in higher trophic levels of the food chain. Green technologies such as phycoremediation is an emerging approach and possess edge over conventional methods to remediate Cd from the environment. The present investigation elucidates the adaptive mechanism of a freshwater microalga, *Scenedesmus* sp. IITRIND2 under Cd stress. The microalga showed excellent tolerance to Cd stress with IC_{50} value of ~32 ppm. The microalga showed phenomenal removal efficiency (~80%) when exposed to 25 ppm of Cd. Such a high uptake of Cd by the cells was accompanied with increased total lipid content (~33% of dry cell weight). Additionally, the elevated level of ROS, lipid peroxidation, glycine-betaine, and antioxidant enzymes evidenced the activation of efficient antioxidant machinery for alleviating the Cd stress. Further, analysis of the fatty acid methyl ester (FAME) presented a steady increase in saturated and polyunsaturated fatty acids with biodiesel properties complying the American and European fuel standards. The study proposes an integrated approach for bioremediation of toxic Cd using hyper-tolerant microalgal strains along with biodiesel production from the generated algal biomass.

1. Introduction

Progressive industrialization and urbanization in the past decades have significantly contributed to elevated levels of various toxic pollutants in the environment. Industrial activities such as mining, refining, electroplating, paints, pigments, fertilizer manufacturing, batteries, etc. are the leading causes for the aggravation of toxic heavy metals (HMs) such as Cadmium (Cd), Arsenic (As), Mercury (Hg), Lead (Pb), etc., in the aquatic ecosystem (Tripathi et al., 2019; Zwolak, 2020). Among these heavy metals, the epidemiological case studies in human beings established that Cd poisoning has exponentially increased over the years (Järup and Åkesson, 2009; Satarug et al., 2003). Considering the severity of Cd poisoning in humans, it has been categorized as group I carcinogen and the minimal permissible limit of Cd in potable water is fixed at 5 ppb (Kinuthia et al., 2020; McElroy and Hunter, 2019). Several existing physicochemical treatment technologies for Cd removal, including adsorption, precipitation, ion-exchange, membrane filtration, etc., suffer from a set of limitations such as lower efficiency, high cost, and generation of secondary wastes (Kanamarlapudi et al., 2018).

Recently, phycoremediation has emerged as an economical, nature-friendly, and efficient alternative compared to conventional techniques for removing heavy metals such as Cd. The ease of cultivation, short generation time, unicellular morphology, and rapid uptake capacity of metals are few imperative properties of microalgae that make its utilization privileged over existing techniques (Doshi et al., 2007; Monteiro et al., 2012). Removal of heavy metals (Cd ions) by microalgae is primarily assisted by the functional groups present on the cell surface that result in biosorption (Monteiro et al., 2012). Further, uptake of Cd ions through ion-channels lead to intracellular sequestration in vacuoles, chloroplast, or mitochondria (Perales-Vela et al., 2006; Yang et al., 2015). Bioaccumulation of Cd ions inside the cells can inflict severe damage to the essential metabolic pathways like photosynthesis, carbohydrate, protein, and lipid biosynthesis. Cd ions potentially disrupt these pathways by displacing the crucial metal ions that act as co-factor to regulate activity of the involved enzymes (Cheng et al., 2016; Lu et al., 2019). Microalgae adapt to Cd/heavy metal stress by modulating their intrinsic defense mechanism comprising of antioxidant machinery, pigments and biochemical components (Perales-Vela et al., 2006).

* Corresponding author. Department of Biotechnology, Indian Institute of Technology Roorkee (IIT-Roorkee), Roorkee, 247667, Uttarakhand, India.
E-mail addresses: krishfbt@iitr.ac.in, mohanpmk@gmail.com (K.M. Poluri).
[1] Present Address: Patel College of Global Sustainability, University of South Florida, Tampa. Florida, 33620

https://doi.org/10.1016/j.chemosphere.2021.131196
Received 14 December 2020; Received in revised form 14 April 2021; Accepted 9 June 2021
Available online 14 June 2021

Further, microalgae also synthesize chelating agents (metallothioneins and phytochelatins) to bind with the excessive Cd ions and regulate the level of oxidative stress inside the microalgae cells (Dean et al., 2019). Further, the generated biomass of microalgae during their growth in Cd supplemented media offers an advantage of proposing a sustainable biorefinery approach.

Additionally, microalgae under such abiotic stress (Cd) also tend to accumulate either carbohydrate or lipid molecules. Microalgae synthesize more lipid content under stress conditions as these lipid molecules act as a sink to sequester excessive ROS generated during encounter of Cd ions (Napan et al., 2015). The Cd present in the biomass can be separated from the biodiesel/FAME (Fatty Acid Methyl Esters) using transesterification process, as Cd gets dissolved in the upper layer of extraction solution containing water and methanolic acid, thus leaving the biodiesel unaffected (Yang et al., 2015). Indeed, an integrated approach combining both heavy metal/Cd removal and biofuel production could also reduce the associated cost of algae biofuels simultaneously with the establishment of efficient heavy metal/Cd treatment technology. Recently, few researchers have employed this integrated approach to remediate As, Cr, Cu, and Pb coupled with triacylglyceride (TAG) accumulation in microalgae cells (Ajayan et al., 2018; Arora et al., 2017a). Similar studies on *Monoraphidium* sp. and *Auxenochlorella protothecoides* have been also performed to understand the effect of Cd stress on lipid synthetic pathway (Lu et al., 2019; Samadani et al., 2018).

To this end, the present study aims to investigate an integrated approach combining bioremediation potential of Cd by freshwater microalga, *Scenedesmus* sp. IITRIND2 and utilization of the biomass for biodiesel production. A comprehensive temporal study has been performed for 12 days to evaluate the changes in biochemical composition of microalgae in order to dissect the alterations in algal physiology that aided in toleration of Cd stress. Various biophysical and biochemical techniques were exploited to decipher the effect of Cd uptake by the microalgal cells. The tolerance mechanism of the microalga was investigated by analyzing the active enzymatic and non-enzymatic antioxidant systems during Cd stress. Furthermore, the suitability of integrating bioremediation with biodiesel production was confirmed by analyzing the fatty acid composition and estimating the biodiesel properties.

2. Material and methods

2.1. Microalga cultivation

The microalga strain *Scenedesmus* sp. IITRIND2 was pre-cultivated in Bold's Basal media (BBM), pH 7.2–7.4 for 7 days. The culture was incubated under light intensity of 200 μmol $m^{-2}s^{-1}$ at 27 °C in shaking condition (180 rpm). The detailed composition of BBM has been mentioned in Table S1-S2.

2.2. Toxicity assessment of Cd

The toxicity of Cd in the microalga was estimated by measuring cell numbers and IC_{50} (inhibitory concentration) of Cd. *Scenedesmus* sp. IITRIND2 in BBM supplemented with Cd in the range 1–100 ppm of $CdCl_2$ were cultivated for 96 h. The culture without Cd was taken as control. The initial cell density was kept at 1×10^5 cells/mL that corresponds to initial OD of 0.3. After 96 h, the cells were appropriately stained with trypan blue and counted using a hemocytometer (Arora et al., 2018). The total cell number (cell/mL) was calculated using the following formula:

Cell number (cells/mL) = (average no. of cells per square*dilution factor) /volume of the square

Further, the IC_{50} of Cd that inhibits the growth of cells by 50% was calculated by plotting a graph between inhibition % and Cd concentration.

2.3. Microalga growth under cadmium toxicity

On the basis of obtained IC_{50} value, growth of *Scenedesmus* sp. IITRIND2 was monitored in the presence of 5, 10, and 25 ppm of $CdCl_2$ supplemented in BBM for 12 days. Media with no-Cd was taken as control. The growth was measured every 48 h by collecting the biomass. The collected biomass was lyophilized before weighing the dry cell weight (DCW).

2.4. Cadmium removal by the microalga

To measure the amount of Cd (ppm) removed by the microalga, 10 ml algal suspension was collected from each flask after every 48 h and centrifuged at 5000 rpm for 10 min. To measure the remaining Cd, the obtained supernatant was passed through 0.45 μm syringe filter and then applied to Inductively-Coupled Plasma Mass- Spectroscopy (ICP-MS, PerkinElmer). The removal percentage of Cd was calculated by the following equation:

$$\% \text{ removal} = ((C_i - C_f)/C_i) * 100$$

Where, C_i and C_f is the initial and final concentration of Cd in the media.

Further, the total Cd adsorbed on the cell surface of microalgae was quantified by treating 100 mg fresh biomass with 10 mM EDTA for 20 min at 150 rpm. The suspension was centrifuged and supernatant was collected to measure adsorbed Cd on the biomass. After EDTA treatment, the pellet was incubated in concentrated HNO_3 and 30% H_2O_2 at 100 °C for 1 h. The digested samples were appropriately diluted and filtered to measure the Cd inside the microalgae cells. Further, bioaccumulation of Cd was confirmed by calculating the bio-concentration factor (BCF) of Cd inside the microalgae cells.

BCF = Total cadmium inside the biomass/ Initial cadmium concentration in the media

2.5. Characterization of Cd interaction with microalgae cells

The interaction of Cd ions with the functional groups present on microalga cell wall was analyzed by Fourier transform infrared spectroscopy (FTIR) (Cary 630, Agilent, USA) within wavebands of 400–4000 cm^{-1}. Lyophilized biomass of control and Cd exposed microalgae cells were directly used for analysis. Further, the net surface charge on control and Cd exposed cells were measured in PBS suspension by recording the zeta potential (ZP) under 80 mV electric field at 25 °C (Zeta sizer, Nano-Z590). In total, 10 independent runs were performed to measure the average ZP by using Malvern software (version 7.03).

The morphological variations due to attachment of Cd on microalgae cells were analyzed by FE-SEM (Field Emission Scanning Electron Microscope) analysis coupled with EDX (Energy dispersive X-ray). In brief, control and Cd exposed algal suspensions were fixed on glass slides with the help of 2.5% glutaraldehyde followed by dehydration in 10–100% ethanol. The samples were sputtered with gold before FE-SEM analysis. Further, the topographical variations on cell surface were analyzed by observing the air-dried samples on glass slide under atomic force microscopy (NT-MDT-INTEGRA, Ireland). The surface roughness was quantitatively estimated by using NovaPX software equipped with AFM.

2.6. Estimation of photosynthetic pigments

Chlorophyll *a*, *b*, and carotenoids were extracted by incubating equal weight of fresh biomass in absolute methanol at 45 °C and 180 rpm for 24 h in dark. After incubation, the supernatant was collected to measure the absorbance at 665, 652, and 470 nm. The pigment content (μg/mL) was determined by equations (Lichtenthaler, 1987).

Chl a (μg/mL) = 16.71*A@665.2–9.16* A@652.4

Chl b (μg/mL) = 34.09*A@652.4–15.28 × A@665.2

Carotenoid (μg/mL) = [(1000 *A@470) – (1.63*Chl a) – (104.9 *Chl b)]

Total chlorophyll = Chlorophyll *a* + Chlorophyll *b*

PS II efficiency = Carotenoid/ (total chlorophyll)

2.7. Quantification of stress markers and osmolytes

2.7.1. ROS species and lipid peroxidation

Intracellular ROS level in microalgae cells were determined by using 2′,7′-dichlorodihydrofluorescein diacetate (H_2DCFDA) dye. Briefly, 1 × 10^7 cells in 50 mM phosphate buffer (pH 7) were mixed with 5 μl of 2 mM H_2DCFDA (in absolute ethanol) in dark for 45 min. The excitation and emission of the samples were recorded at 485 nm and 520 nm, respectively (Yilancioglu et al., 2014). Further, total TBARS (thiobarbituric acid reacting substance) content was estimated to evaluate the lipid peroxidation in cells. Briefly, 0.05 g of fresh biomass was crushed with liquid N_2 in 0.1% TCA (trichloroacetic acid). 500 μl of TCA extract was mixed with an equal volume of 20 mM TBA (made in 0.1% TCA) and heated for 45 min at 95 °C (Arora et al., 2017b). The following equation was used for estimating the total TBARS content.

TBARS content = $(A_{532} - A_{600})$/EC

Where, EC is the extinction coefficient of abduct formed = 155 $mM^{-1}cm^{-1}$.

2.7.2. Osmoprotectants

Total proline content in Cd exposed microalga cells was estimated using a standard curve of L-proline ranging from 0 to 50 μg/mL. The fresh weight of cells (0.05 g) was homogenized in 3% sulfosalicylic acid. Soluble content was extracted in toluene, and absorbance was taken at 520 nm (Bates et al., 1973). The same amount of fresh weight was collected for estimating glycine betaine complex in microalgae cells. Briefly, cells were homogenized in an equal volume of 2 N H_2SO_4: deionized water (200 μl) and incubated at 4 °C for 2 h. Further, chilled KI−I_2 reagent was added and incubated for 16–18 h below 5 °C (Valadez-bustos et al., 2016). Total glycine betaine content was extracted in 1, 2-dichloroethane and measured by taking absorbance at 365 nm.

2.7.3. Total antioxidant by ABTS (2,2-Azino-bis-(3-ethylbenzothiazoline-6-sulfonic acid)) assay

The antioxidant capacity of microalgal extracts was estimated by performing ABTS scavenging assay as per the protocol by (Belghith et al., 2016). Dithiothreitol (DTT) was used as a standard for measuring the reduction of the ABTS cation radicals at 30 °C. Briefly, methanolic extract (5 mg/mL) was mixed with an activated solution followed by overnight incubation. The activated solution consists of an equal volume of ABTS (7 mM) and potassium persulfate (2.45 mM). The decrease in the absorbance was recorded at 734 nm after mixing the algal extract and activated solution.

2.7.4. Antioxidant enzymes

The enzymatic extract of Cd spiked and control cells was prepared in lysis buffer to measure catalase (CAT), glutathione reductase (GR), and ascorbate peroxidase (APX) activity. CAT activity was evaluated by observing the fall in absorbance at 240 nm for 3 min where, extinction coefficient is equal to 0.0436 mM/cm (Arora et al., 2017b). The reaction mixture (1 ml) constitutes 0.8 ml of phosphate buffer and 0.1 ml of H_2O_2 (10 mM). GR activity was estimated by monitoring the conversion of NADPH (10 Mm) to NADP in the presence of glutathione disulfide (GSSG) (10 mM). The absorbance was measured at 340 nm taking 6.22 mM/cm as extinction coefficient (Schaedle and Bassham, 1977). GR activity was calculated by recording the reduction in absorbance. The reaction mixture containing 0.69 ml of phosphate buffer, 0.1 ml of each H_2O_2, ascorbic acid, and EDTA was used to measure the APX activity. The gradual decline in absorbance was measured at 290 nm and extinction coefficient of 2.8 mM/cm was used for further calculation. One unit of enzyme activity is defined as the consumption of 1 μmol substrate per minute and presented in terms of specific activity (Unit/mg protein). SOD activity was performed according to the method previously established by Gao et al., 2005). One SOD unit is equal to the quantity of enzyme required for inhibiting photoreduction of nitro-blue tetrazolium (NBT) by 50%.

2.8. Estimation of total carbohydrate, soluble protein, and lipid content

Estimation of total carbohydrate was done by phenol sulfuric acid method. 10 mg lyophilized biomass was subjected to sulfuric acid treatment at 100 °C for 1 h. The obtained solution was filtered and used for estimating carbohydrate by taking glucose as standard. Total soluble protein was estimated by the Bradford method utilizing BSA as standard. Briefly, 5 mg biomass was lysed with mortar pestle in 1 ml lysis buffer (Arora et al., 2019). Further, Nile red stained cells were observed under the Fluorescence microscope to confirm the presence of lipid bodies. Total lipid from microalgae biomass was recovered in chloroform: methanol (2:1) solution and weighed gravimetrically (Bligh and Dyer, 1959). The equations mentioned below were used to quantify the total lipid content (%) and lipid productivity respectively:

Lipid content = (Dry weight of total extracted lipid/ weight of dry biomass) *100

Lipid productivity (mg/L/day) = Biomass productivity (mg/L/day) *(lipid content (%)/100)

2.9. FAME (fatty acid methyl ester) profiling and biodiesel properties

The extracted lipid was transesterified in methanolic H_2SO_4 at 90 °C for 1 h. The samples were brought at room temperature and mixed with hexane and distilled water (1:2). Further, the lower phase containing FAME was aspirated out and utilized for GC-MS (Gas chromatography-Mass spectrometry) analysis by using helium as carrier gas. DB5 capillary column (split-less mode) was used to separate the constituent components. The samples at flow rate of 1 ml/min were injected (1 μl) at 250 °C. The initial oven temperature (50 °C) was gradually raised to 180 °C at the rate of 25 °C/min for 1 min, then 220 °C (10 °C/min) and eventually to 250 °C (15 °C/min) for 15 min (Arora et al., 2016). The ion source was maintained at 230 °C for detecting fatty acids. The biodiesel properties including saponification value (SV), iodine value (IV), cetane number (CN), long chain saturation factor (LCSF), degree of unsaturation (DU), oxidative stability (OS), cold flow plugging property (CFPP), high heating value (HHV), and kinematic viscosity (KV) were estimated by empirical formulas as mentioned in Table S2.

2.10. Analysis of statistical significance

All the experiments were performed thrice and the data is represented in mean ± standard deviation. GraphPad Prism V5.0 was used to analyze the statistical significance by using One-way ANOVA followed by Tukey's test. The p-values < 0.05, 0.01, and 0.001 were shown with *, ** and ***.

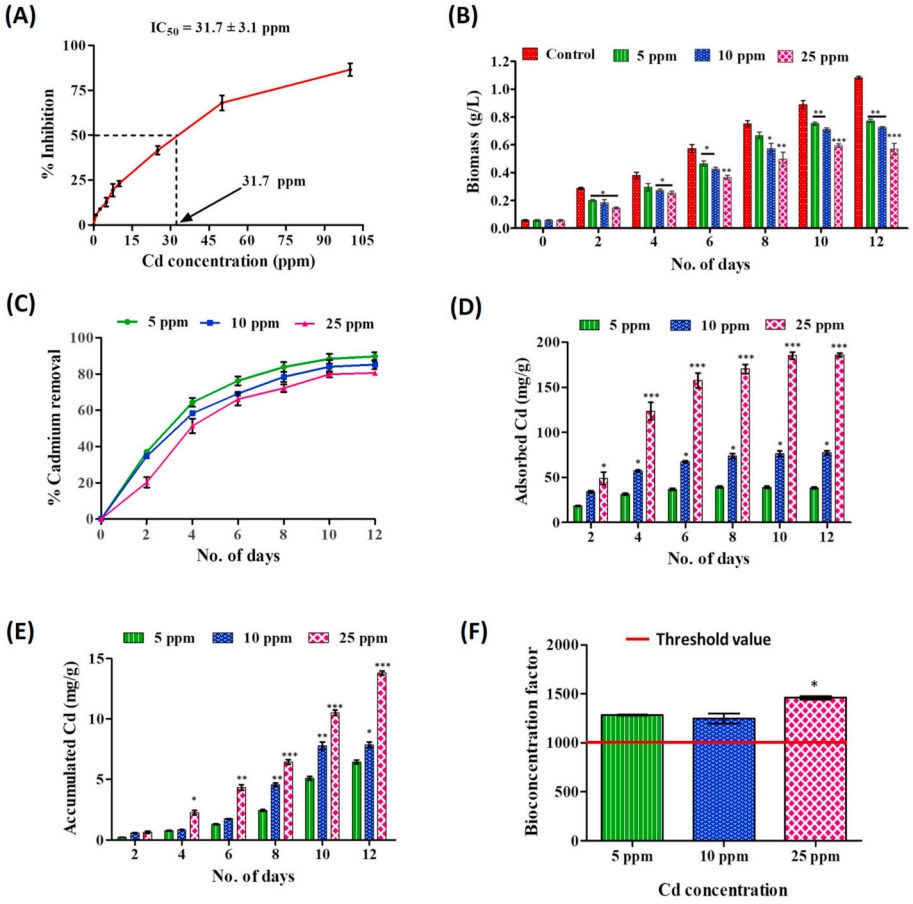

Fig. 1. (A) IC_{50} value of Cd for *Scenedesmus* sp. IITRIND2 after 96 h of exposure; **(B)** Dry cell weight of *Scenedesmus* sp. IITRIND2 recorded every 48 h up to 12 days; **(C)** Time-dependent removal percentage of cadmium from media; **(D)** Time dependent quantification of adsorbed Cd content on algal cell surface; **(E)** Time dependent quantification of accumulated Cd content inside the microalga; **(F)** Bioconcentration factor for *Scenedesmus* sp. IITRIND2 in tested Cd concentrations (5, 10 and 25 ppm) after 12 days of incubation.

3. Results and discussion

3.1. Tolerance and removal of cadmium by Scenedesmus sp. IITRIND2

The extent of toxicity of a given compound/metal on a given organism can be estimated by measuring its growth inhibition features. IC_{50} value represents the concentration of the toxicant responsible for inhibiting the growth of cells by 50%. To assess the toxicity of Cd on *Scenedesmus* sp. IITRIND2, IC_{50} value was determined by measuring the growth of the algae at various concentrations (0–100 ppm) of this heavy metal. At 96 h time period, the IC_{50} was found to be 31.7 ± 3.1 ppm (Fig. 1A). Comparing the IC_{50} of *Scenedesmus* sp. IITRIND2 to those of the earlier reported studies suggested that this algal strain has high tolerance towards Cd stress (Table S4). To date, the maximum IC_{50} of 20.9 ppm for Cd has been reported for *Scenedesmus* sp. (Duque et al., 2019).

Based on the obtained IC_{50} value, *Scenedesmus* sp. IITRIND2 was cultivated in BBM supplemented with varying concentrations of Cd (5, 10 and 25 ppm) for 12 days to monitor the biomass production (Fig. 1B). The data suggested that the cells showed concentration dependent inhibition in biomass production for Cd stressed cells. Among all the tested concentrations, cells cultivated in 25 ppm of Cd exhibited maximum reduction (~ 50%) in biomass during first 2 days, which was followed by 10 ppm and 5 ppm cultures. All the *Scenedesmus* sp. IITRIND2 cultures entered the exponential phase on day 2 of growth; however, a slower growth rate was observed in Cd spiked cells. The exponential phase lasted for 9 days (day 2 - day 10) in control cells, whereas Cd spiked cells showed reduced span of log phase (6 days). The onset of stationary phase was characterized by no significant increase in dry cell weight (DCW) after day 8 in Cd spiked cells, whereas day 10 in control cells. After incubation of 12 days, maximum biomass production was observed in control cells (1.07 ± 0.09 g/L) followed by cells cultivated in 5 ppm (0.77 ± 0.02 g/L), 10 ppm (0.72 ± 0.01 g/L) and 25 ppm (0.57 ± 0.04 g/L) Cd. The observed reduction in biomass was also visible from the color of Cd spiked cultures (Fig. S1). Several other studies have also reported the inhibitory action of Cd on the growth of different microalgae (Belghith et al., 2016; P.S et al., 2020; Zhao et al., 2019). For instance, *Chlorella vulgaris* showed more than 50% inhibition of growth in the presence of 7 ppm Cd in media (Cheng et al., 2016).

The microalga was able to maintain its growth and survival in presence of Cd, hence it was further evaluated for its removal efficacy. The time course removal profile of Cd from media containing initial concentrations of 5, 10 and 25 ppm has been presented in Fig. 1C. The data suggest that removal of Cd increased with time, and reached a plateau at day 10 in all the tested concentrations. Around ~50–60% removal was observed in all the tested conditions during initial 4 days. The data suggested that by 12th day ~80% (~20 ppm) of Cd has been efficiently removed at its highest concentration of 25 ppm present in the medium. At low initial concentrations (~5 ppm) of Cd, the cells have efficient removed ~ 90% (~4.5 ppm) of Cd. Moreover, the recorded removal efficiency of *Scenedesmus* sp. IITRIND2 was exceptionally high in comparison to other microalgae species like *Tetraselmis suecia, Scenedesmus, Chlorella* etc., (Table S4) (Duque et al., 2019; P.S et al., 2020; Pérez-Rama et al., 2002).

Microalgae cells remove heavy metals from media by a combined action of biosorption (extracellular) and bioaccumulation (intracellular). Biosorption involves the attachment of metal ions on the surface by virtue of functional groups. After attachment these metal ions are further internalized and get accumulated inside the cells (Samadani et al., 2018). To understand the key phenomenon responsible for removal of Cd ions by *Scenedesmus* sp. IITRIND2, it is essential to quantify the portion of Cd ions removed extracellularly and

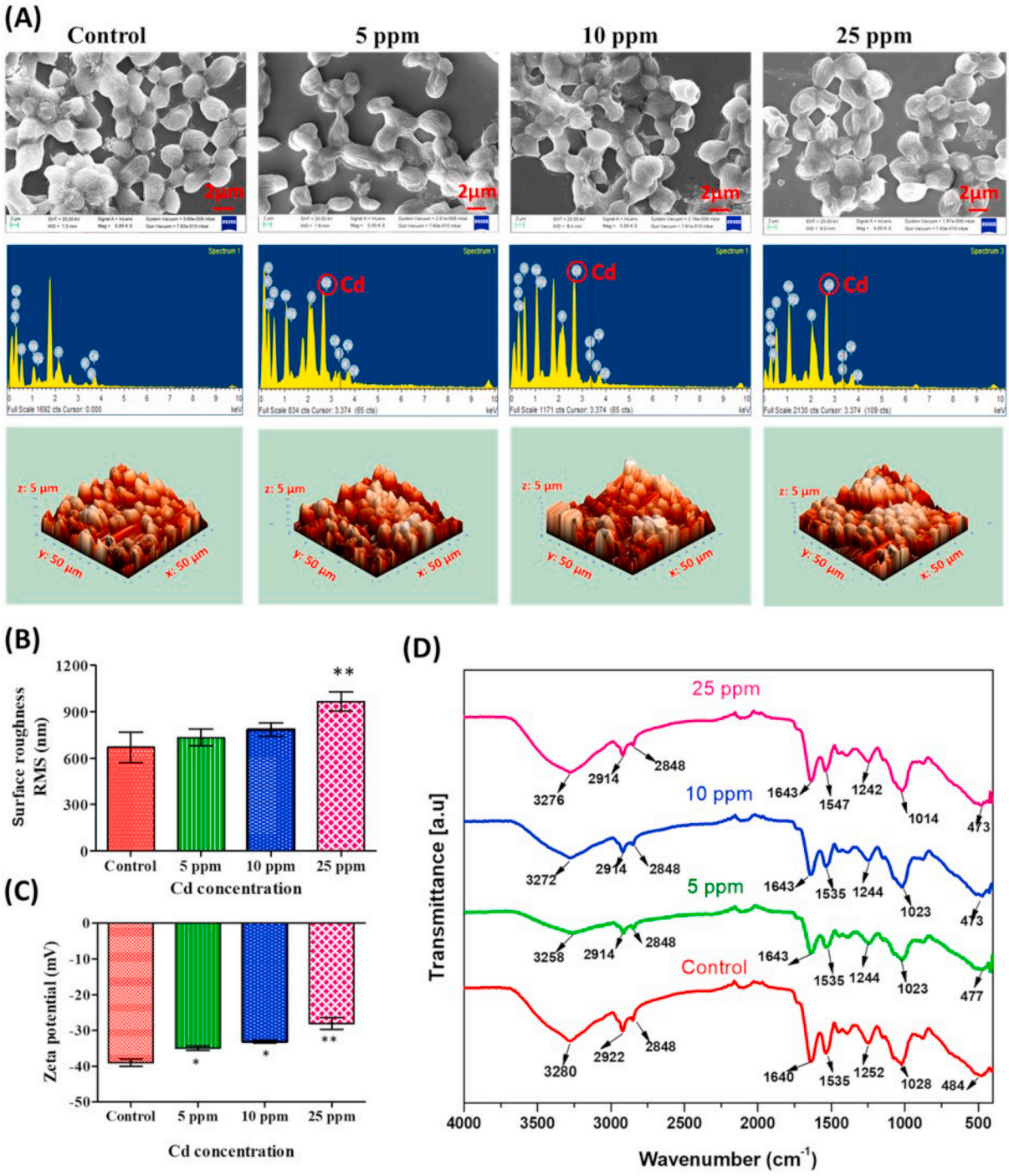

Fig. 2. (A) FE-SEM images at 2 μm scale bar; magnification 5,000× (Top panel), EDX analysis of cell surface showing the adsorption of Cd ions (middle panel), and 3-D AFM images (x and y axis having scale of 50 μm and z-axis of 5 μm) (bottom panel) of control and cadmium exposed microalgae cells; **(B)** Surface roughness by AFM analysis; **(C)** Zeta potential; and **(D)** FTIR analysis of control and Cd spiked microalgae cells after 12 days of incubation.

intracellularly. The time course quantification of extracellular Cd attached on the microalgae cell surface and Cd accumulated inside the cells are presented in Fig. 1D and E. The data suggested that the cells showed rapid biosorption of Cd during initial 4 days and eventually attained a constant value at the later stage of incubation. Initially the Cd ions get rapidly adsorbed on the cell surface, and slowly get internalized inside the cells after certain time point. The maximum adsorbed (186 ± 2 mg/g) and accumulated (14 ± 0.2 mg/g) Cd content was observed for cells cultivated in 25 ppm Cd. Similarly, 10 ppm Cd cultures showed higher adsorption (77 ± 2 mg/g) and accumulation (8 ± 0.2 mg/g) in comparison to 5 ppm Cd cultures (38 ± 1 mg/g; 6.4 ± 0.2 mg/g).

The experimental results obtained in the current study established that biosorption contributes to the significant portion of removed Cd from the media as compared to bioaccumulation. On a similar note, rapid biosorption of Cd was observed in *Chlamydomonas reinhardtii*, *Tetraselmis suecica*, *Dunaliella salina*, *Scenedesmus acutus* and *Chlorella pyrenoidosa* (Belghith et al., 2016; P.S et al., 2020; Pérez-Rama et al., 2002; Samadani et al., 2018). Further, accumulation of Cd inside *Scenedesmus* sp. IITRIND2 cells was also substantiated by analyzing the bioconcentration factor (BCF) after 12 days. The obtained values of BCF

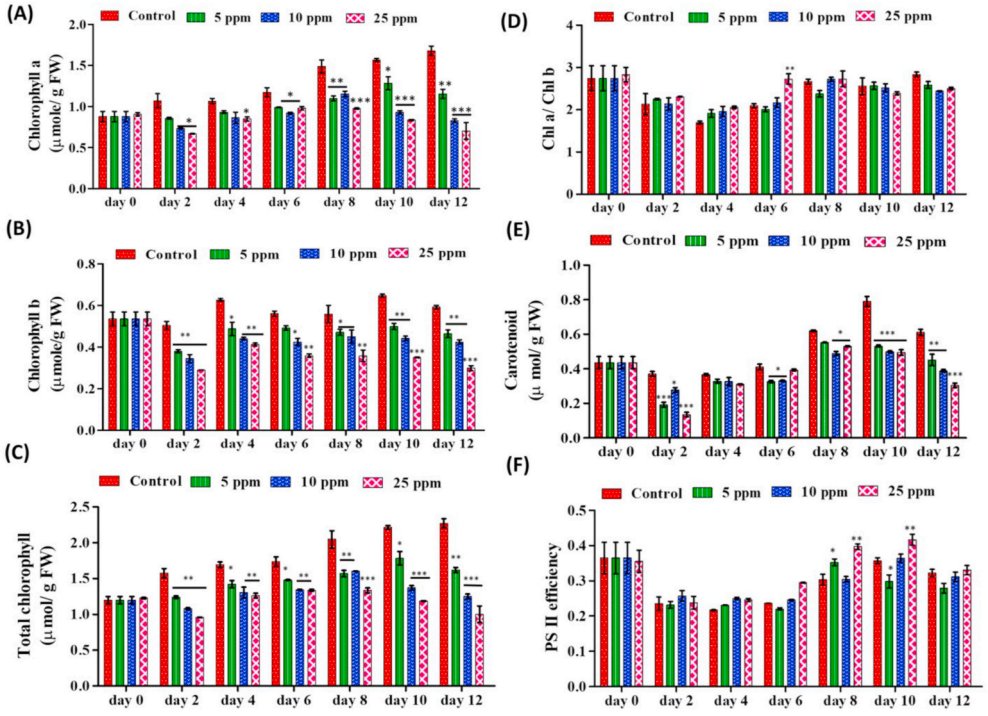

Fig. 3. (A) Chlorophyll *a*; **(B)** Chlorophyll *b*; **(C)** Total Chlorophyll; **(D)** Ratio of Chlorophyll *a* to Chlorophyll *b*; **(E)** Carotenoid content; and **(F)** PS II efficiency of *Scenedesmus* sp. IITRIND2 recorded every 48 h under different Cd concentrations (5, 10, 25 ppm) up to 12 days.

were >1000 in all the Cd spiked cultures, indicating that *Scenedesmus* sp. IITRIND2 is a hyperaccumulator of Cd metal **(**Fig. 1F**)** (Zhu et al., 1999).

3.2. Characterization of surface morphology of cadmium exposed microalga cells

The biosorption of Cd on the cell surface could cause some notable morphological changes like an increase or decrease in cell size, appearance of ridged surface topography, etc. The morphological variations on the cell surface due to Cd toxicity were visualized by FE-SEM analysis and confirmed by EDX (energy-dispersive X-ray) analysis. The SEM images showed no significant variation in the cell size, but surface aberrations were visible in the Cd spiked cells. Further, EDX analysis showed prominent peaks of Cd confirming its adsorption on the cell surface, which led to the rough and ridged cell surface of Cd spiked cells in comparison to control cells (Fig. 2A). In addition to this, the AFM analysis was performed to obtain detailed visual insights into the surface topography of the cells. The quantitative estimation of topographical changes in the cell surface was denoted by the increased root mean square (RMS) value of surface roughness in Cd spiked cells (Fig. 2B). The maximum RMS value of ~ 966 nm was observed in 25 ppm Cd cells, which was ~ 1.4 fold higher than in control (~ 677 nm). Similar results were obtained for *Ochrobactrum anthropi* where bioaccumulation of chromium (Cr) led to an increased surface roughness of the cells either due to strong binding of metal ligands or upon rupture of cells in response to toxic metal ions (Li et al., 2008).

Further, a reduction in zeta potential (cell surface charge) with an increase in Cd concentration also validated the binding of Cd ions on the cell surface. The zeta potential decreased from −38 mV in control to −29 mV in 25 ppm Cd spiked culture after 12 days (Fig. 2C). It has been reported that the binding of divalent cations such as Cu^{2+} and Cd^{2+} present in the growth media reduces the negative potential in *Dunalliela* sp. (Gimmler et al., 1991).

To study the interaction of Cd ions with the microalgae cell wall, FTIR study was performed. The cell surface of microalgae comprises of prominent functional groups, namely, –COOH, $–NH_2$, - PO_3, $–SH_2$, and –OH that help in metal adherence and lead to its detoxification (Arora et al., 2018). The FTIR spectra of *Scenedesmus* sp. IITRIND2 exposed to different concentrations of Cd indicated notable peak shifts in comparison to control (Fig. 2D). For instance, distinct peak at 3280 cm^{-1} in control and its shift to 3558 cm^{-1} in Cd spiked cells represent changes in O–H stretching (P.S et al., 2020). Further, interaction of Cd ions with aliphatic C–H and aldehyde C–H was confirmed with a peak shift from 2922 cm^{-1} in no Cd cells to 2914 cm^{-1} in Cd spiked cells. Similarly, peak shift from 1535 cm^{-1} in control cells to 1547 cm^{-1} in 25 ppm Cd cells highlighted the involvement of N–H bending, which generally represents the protein amide (II) bond (Shanmugam et al., 2012). Furthermore, interaction between phosphate groups on cell wall and Cd ions was confirmed by stretched phosphodiester bonds (>P═O) representing the peak shift from 1252 cm^{-1} to 1244 cm^{-1} (D'Souza et al., 2008). The overall spectral changes in Cd treated cells represent the possible interaction of metal ions with amino, amide, and anionic functional groups on the algae cell surface.

3.3. Attenuation of photosynthetic pigments in response to cadmium stress

Photosynthesis machinery is the most vulnerable target of any metal-induced stress (Pfeiffer et al., 2018). Cd ions can potentially hamper the photosynthetic performance of microalgae cells by replacing the Mg ions in chlorophyll (Arunakumara and Zhang, 2007). To elucidate the changes in the microalgae photosynthetic system, chlorophyll *a*, *b*, carotenoid and PS II efficiency were analyzed under Cd stress. The data suggested that chlorophyll *a* dropped significantly on day 2 under Cd stress conditions during initial adapting phase, which later onwards showed a consistent recovery. However, the total chlorophyll *a* content in the Cd stressed cells was significantly lower by 30–55% respectively with respect to control cells on 12th day (Fig. 3A). Similar pattern was observed for chlorophyll *b*, and total chlorophyll (a+b) content. It has been observed that the content of chlorophyll *b* and total chlorophyll (a+b) reduced by 25–50% in Cd spiked cells by the end of 12th day (Fig. 3B–C). A constant ratio of chlorophyll *a*/b has been obtained indicating that both chlorophyll *a* and chlorophyll *b* were similarly

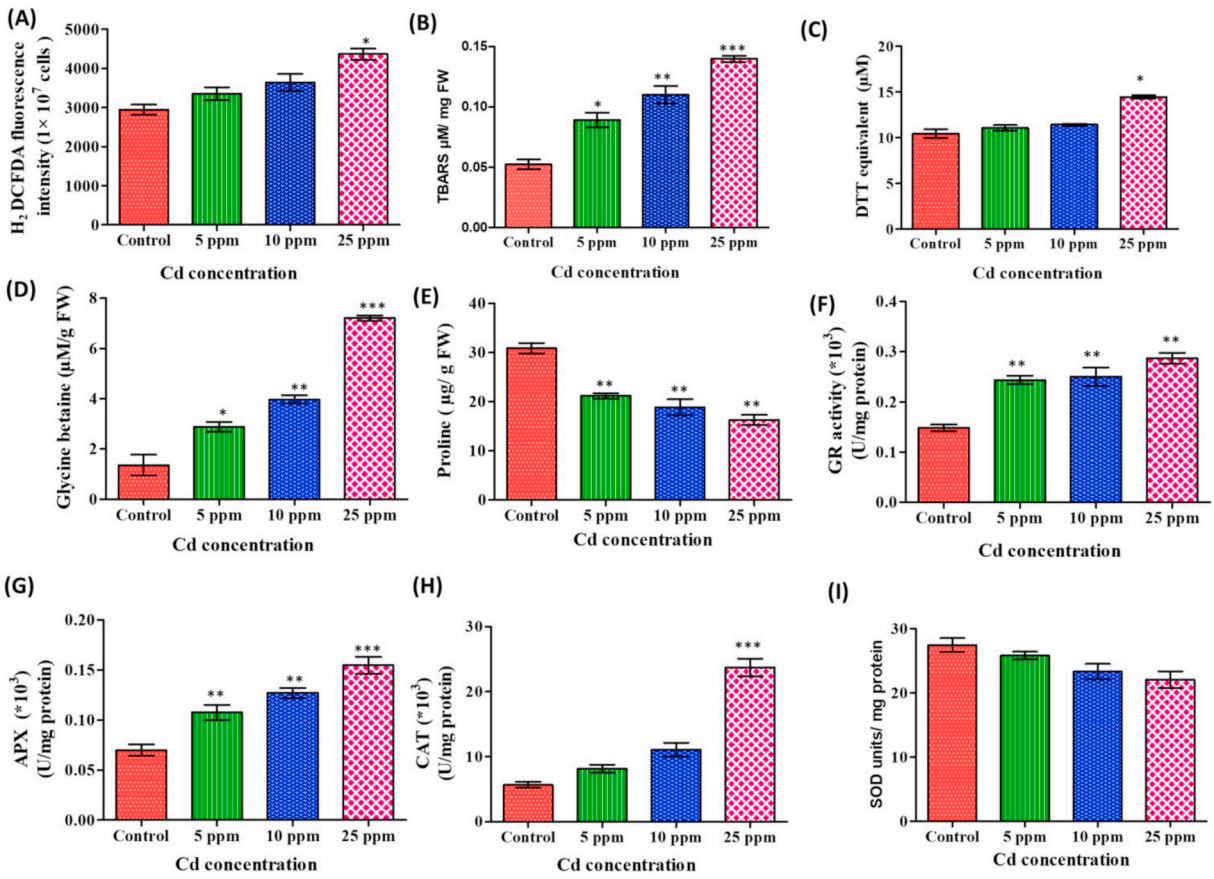

Fig. 4. Changes in (A) Total ROS in terms of H_2DCFDA fluorescence; (B) lipid peroxidation in terms of TBARS content; (C) total antioxidants in terms of DTT equivalent; (D) total glycine betaine; (E) proline content; (F) Glutathione reductase (GR) activity; (G) Ascorbate peroxidase (APX) activity; (H) Catalase activity; and (I) Superoxide dismutase (SOD) activity.

attenuated under Cd stress (Fig. 3D). Overall, the data suggested that the synthesis of chlorophyll changed in a time dependent manner in both control and Cd spiked cells. Further, the toxic effect of Cd ions was clearly evident with the reduced chlorophyll content observed in Cd spiked cells in later stage of growth. Interestingly, chlorophyll content in control cells did not showed any reduction till day 12, which could be attributed to the increased rate of chlorophyll synthesis in late growth phase. Chlorophyll synthesis in microalgae depend on the stage of the growth and also on the amount of light intensity reaching to each of the cells. During growth , as the cell density increases, the cells face shading effect where due to higher biomass, less intensity of light is available to each cell. This in turn lead to reduced photosynthesis for formation of starch but increased synthesis of compounds like chlorophyll a as observed in the present case (da Silva Ferreira and Sant'Anna, 2017).

Carotenoids play crucial role in protecting the unsaturated lipids from peroxidation under stress conditions (Zhang et al., 2013). The analysis of carotenoid content in microalgae cells cultivated under 5, 10, and 25 ppm Cd highlighted significant accumulation of carotenoids in all cultures by day 8, which remained constant for the rest of the incubation time. In comparison to control, the Cd spiked cells encountered ~ 37–46% decline in carotenoid content by 12th day of incubation (Fig. 3E). However, the data on PS II efficiency did not represent any significant changes among control and Cd spiked cells on 12th day (Fig. 3F). The constant values of chlorophyll *a*/b and carotenoid/total chlorophyll suggested that *Scenedesmus* sp. IITRIND2 was capable to adapt itself under Cd stress by maintaining a balance between the biosynthesis of pigment to protect the photosynthetic machinery from oxidative damage. These results are in line with previous reports on *Monoraphidium* sp. QLY-1 and *Chlorella vulgaris* where Cd stress inhibited synthesis of chlorophyll *a b*, and carotenoid biosynthesis (Cheng et al., 2016; Zhao et al., 2019).

3.4. Alterations in stress metabolites and antioxidant system of microalgae under Cd exposure

The oxidative metabolism in the cells leads to the production as well as removal of ROS in a regulated manner (Zhu et al., 2019). Accumulation of Cd ions inside the cells generate excessive ROS that can hamper the cell membrane integrity by inducing lipid peroxidation (Piotrowska-Niczyporuk et al., 2012). To regulate the extent of oxidative damage caused due to ROS, microalgae cells activate their antioxidant machinery comprising both metabolites/osmolytes and enzymes (Sytar et al., 2013; Tripathi et al., 2021a,b). To unveil the survival mechanism adopted by the cells under Cd toxicity, modulation in stress metabolites (ROS), osmolytes (glycine-betaine and proline), and activity of antioxidant enzymes GR (glutathione reductase), APX (ascorbate peroxidase), CAT (catalase), and SOD (superoxide dismutase) were investigated.

The data obtained for cellular ROS indicated that cell cultivated in 10 and 25 ppm Cd spiked cells represent ~ 1.3–1.5 fold rise in the H_2DCFDA fluorescence intensity, whereas 5 ppm Cd cells does not show any significant change (Fig. 4A). The level of TBARS content increased by ~ 1.4–3 fold in all 5, 10, and 25 ppm Cd spiked cultures thus confirming the generation of oxidative stress in cells (Fig. 4B). To ameliorate the ROS toxicity, microalgae cells produce antioxidant molecules along with small osmolytes such as proline and glycine betaine (GB) (Arora et al., 2017b). The total antioxidant activity measured in terms of DTT equivalent does not represent any significant rise in 5 and 10 ppm Cd cultures, whereas ~ 1.5 fold increase was observed in 25 ppm Cd cultures (Fig. 4C). Further, estimation of osmolytes (GB and proline) revealed that Cd spiked cells accumulated significant amount of GB

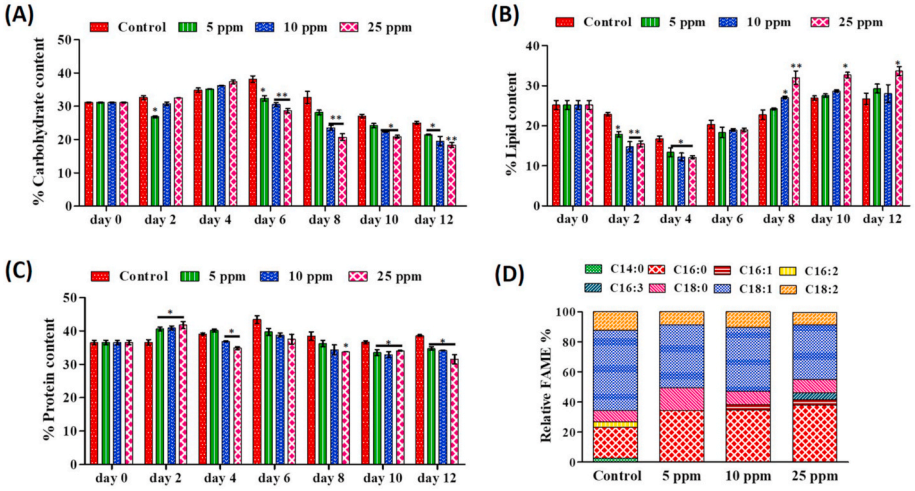

Fig. 5. Effect of different cadmium concentration on (A) total carbohydrate content (%); (B) total lipid content (%); (C) total soluble protein (%) and; (D) FAME profile of control and cadmium spiked biomass after 12 days of incubation.

corresponding to ~ 2–4 fold rise in comparison to control (Fig. 4D). On contrary, opposite trend was followed by proline accumulation, where ~ 1.5–2 fold decline was observed in 5, 10, and 25 ppm Cd exposed cells (Fig. 4E). In line with these observations, Dhir et al. reported a reduced proline content in *Ceratophyllum*, *Wolffia*, and *Hydrilla* in presence of Cd (Dhir et al., 2004). Similarly, decline in proline content was also observed in *C. vulgaris* cells when exposed to higher concentration of Cu (>2.5 μM) or Cr (>5 μM) (Mehta and Gaur, 1999).

Increase in proline and glycine betaine components have been widely reported in different microalgae to confer tolerance to heavy metals as they can act as osmoprotectants, metal chelators and/or ROS quencher etc. (Hossain et al., 2015; Liang et al., 2013; Sharma and Dietz, 2006). The possible reason of depletion in proline content might be related to the substrate unavailability for proline. Under heavy metal stress in cells, glutamate is rapidly utilized to maintain the GSH (glutathione) pool and eventually contribute in the formation of phytochelatin to chelate excess metal ions (Hossain et al., 2012). It might also be possible that under Cd stress *Scenedesmus* sp. IITRIND2 prefer formation of phytochelatin rather than proline, thus regulating the proline attenuation. The overall results suggested that GB conferred tolerance to Cd toxicity in *Scenedesmus* sp. IITRIND2 to imbibe high ROS levels, and to maintain the osmotic balance inside the cells.

The enzymatic antioxidant system comprises of APX, CAT, GR, and SOD which play a crucial role in managing excessive oxidative stress. Further assessment of the enzyme-based antioxidant machinery of *Scenedesmus* sp. IITRIND2 revealed that GR and APX activity increased by ~ 1.5–2 fold and ~ 1.5–3 folds in 5, 10, and 25 ppm Cd cells respectively (Fig. 4F–G). In contrast to this, significant increase in CAT activity (~ 5 fold) was only observed in 25 ppm Cd cultures (Fig. 4H). Interestingly, no significant changes were observed in SOD activity of Cd spiked cells (Fig. 4I). The results obtained were in agreement with the earlier reports where Cd stress in *C. vulgaris* and *D. salina* led to higher activity of GR, APX and CAT (Cheng et al., 2016; Zhu et al., 2019).

The higher activity of GR in Cd spiked cells suggests the enhanced GSH level in the cells. GSH itself or by further forming phytochelatins help to chelate the excess Cd ions in the subcellular compartment of cells and relieves the oxidative burden (Balzano et al., 2020; Kováčik et al., 2017; Tripathi et al., 2021a,b). In addition, GSH also detoxifies hydrogen peroxides (H_2O_2) by taking part in glutathione-ascorbate cycle (Cheng et al., 2016). This metabolic cycle is primarily involved in detoxification of ROS species by involving GSH, ascorbate and NADPH, by the action of APX, monodehydroascorbate reductase and dehydroascorbate reductase along with GR (Hasanuzzaman et al., 2019). Thus, the significant rise in GR and APX activity of Cd stressed cells highlights the combined action of these enzymes in detoxifying ROS. The overall variations in activities of enzyme-based antioxidant systems suggest that the defense system is being active inside the cell that is responsible for relieving the stress to support the survival of *Scenedesmus* sp. IITRIND2 under Cd toxicity.

3.5. Alterations in the total lipid, carbohydrate and soluble protein in cadmium spiked microalgal cells

Microalgae are capable of adjusting their carbon flux towards synthesis of storage molecules such as carbohydrates and lipids to inhabit themselves under various stress conditions. To analyze the detrimental effect of Cd toxicity on microalgae, temporal analysis of *Scenedesmus* sp. IITRIND2 biochemical components (carbohydrate, lipid, and protein) was performed for 12 days. The total carbohydrate content of *Scenedesmus* sp. IITRIND2 in all the cultures increased up to day 6 and reached a maximum value of 38.1 ± 2.0% in control, after which a steady decline in carbohydrate content was observed indicating a bell-shaped curve. In control cultures, at initial stages of growth, carbohydrate is the primary product of photosynthesis in microalgae cells that is rapidly accumulated and is utilized for other essential metabolic activities like DNA replication, nuclear division, cytokinesis etc., (Vitova et al., 2014). However, as the growth proceeds towards the end of exponential phase, starch degradation takes place and the carbon skeleton is fluxed towards lipid biosynthesis (Laurens et al., 2014; Sharma et al., 2012). Similarly, by the end of 12th day, ~ 1.4 fold decline in carbohydrate content was observed for Cd spiked cells in comparison to control cells (25.0 ± 1.7%) (Fig. 5A). The decrease in total carbohydrate content under Cd stress could be explained by the possible inhibition of carbon metabolism due to the interaction of Cd with reactive sites of essential enzymes such as ribulose biphosphate carboxylase (Stiborová et al., 1987). The time-course estimation for lipid content revealed that 25 ppm Cd spiked cultures exhibited a significant rise in lipid accumulation during day 8 - day 12 and attained ~ 1.3 fold higher lipid content (%) as compared to control (Fig. 5B). Further calculation for lipid productivity revealed that Cd spiked cells exhibited a decline in comparison to control. The control cultures having lipid productivity of 24 ± 1.2 mg/L/day was followed by 5 ppm (19 ± 2 mg/L/day), 10 ppm (17 ± 1.5 mg/L/day), and 25 ppm (16 ± 1.7 mg/L/day). The observed decline of 21%, 28%, 33% in the presence of 5, 10, 25 ppm Cd can be directly attributed to the decrease in algal biomass due to Cd toxicity. Indeed, the lipid productivity can be enhanced by adapting a continuous mode of cultivation as reported by Lu et al. in a recent study. The authors showed 1.5- and 1.3-fold increase in biomass of *Chlorella vulgaris* exposed to 0.5 and 1 mg/L Cr (VI)

Table 1
Comparative analyses of biodiesel properties of Fatty Acid Methyl Esters from *Scenedesmus* sp. grown in different concentrations of cadmium with ASTM D6751, EN 14214 (Knothe, 2006) fuel standards and plant oil methyl esters (Ganapathy et al., 2009; Ramos et al., 2009).

Physical properties	Standard fuel parameter		Control	Cadmium exposed cells			Plant oil methyl esters	
	ASTM (D6751-02)	EN (14214)	BBM	5 ppm	10 ppm	25 ppm	JME	PME
Saponification value (mg KOH)	–	–	120	130	140	150	96	49
Iodine value (g I_2/100 g)	–	120 (max)	46	32	43	53	–	–
Cetane number	47 (min)	–	78	80	75	69	54	61
Degree of unsaturation (% weight)	–	–	51	35	44	51	–	–
Long Chain Saturation Factor (% weight)	–	–	3.6	4.8	4.8	5.1	–	–
High heating value (MJ/kg)	–	–	44	44	43	43	–	–
Cold flow plugging property (°C)	–	≤5/≤ −20	−4	−1	−1	−5	−2	13
Kinematic viscosity (mm^2/s)	1.9–6.0	3.5–5.0	3.7	2.7	2.5	2.8	4.3	4.4
Oxidative stability (h)	–	>6	19	25	18	19	3.9	16.5

respectively, when cultivated in a continuous membrane photobioreactor, in comparison to batch cultivation (Lu et al., 2021). Adopting such continuous cultivation methods can further enhance the overall lipid productivity of Cd spiked *Scenedesmus* sp. IITRIND2 by increasing its biomass production.

The quantitative data on lipid content was confirmed by Nile red staining images of the control and Cd spiked microalgal cells. The cells under Cd stress emitted brighter yellow color fluorescence as compared to control, thus confirming the enhanced accumulation of lipid droplets (Fig. S2). Further analysis for total protein content illustrated a significant rise in Cd spiked cells during the initial adaptive phase, which eventually encountered ~1.3 fold decline by the end of 12th day (Fig. 5C). A significant increase in protein content in Cd spiked cells on day 2 suggests the expression of metal-binding factors or chelating agents responsible for reducing the availability of the free ions (Fig. 5C). A similar increase in protein content was also reported in *Monoraphidium* cells spiked with Cd (Zhao et al., 2019). The long-term incubation of 12 days representing a significant decrease in protein content might be due to the fragmentation of proteins by the induced ROS and oxidative stress (John et al., 2008). Moreover, reduction in photosynthetic rate also contributes in lowering the protein content due to limited supply of carbon (Afkar et al., 2010). However, slight reduction in protein content of control cells could be attributed to the nutrient limitation and reduced photosynthesis in later phase of growth, where cells start to reduce the protein build up and catabolize proteins to synthesize storage molecules like neutral lipids (Shaikh et al., 2019). The temporal changes in the biochemical composition analyzed in the present study evidenced that under Cd stress, *Scenedesmus* sp. IITRIND2 initially accumulated carbohydrates for stress mitigation, and later it reallocated its carbon flux towards lipid biosynthesis in the late phase of growth. Moreover, decline in protein content also contributed to the lipid synthesis. Similar results were reported for *Dunaliella* sp. and *Scenedesmus rotundus*, where Cd stress led to a significant decrease in carbohydrate and protein content (Belghith et al., 2016; Shivaji and Dro, 2019).

3.6. FAME profiling and estimation of biodiesel properties

Scenedesmus sp. IITRIND2 accumulated significant quantity of neutral lipid under Cd stress; hence it is essential to analyze its fatty acid composition. The primary constituents of FAME in control culture were contributed by methyl ester chain of C16 and C18 having a highest portion of C18:1 (oleic acid) followed by C16:0 (palmitic acid), C18:2 (linoleic acid), C18:0 (stearic acid), C16:2 (hexadecadienoic acid) and C14:0 (myristic acid) (Fig. 5D). The FAME composition of the microalgae cultivated under 5, 10 and 25 ppm Cd exhibited prominent variation in their profiles in comparison to control. The relative quantities of saturated fatty acids (C16:0, C18:0) increased under all Cd spiked cultures. The content of palmitic acid (C16:0) increased by ~ 1.7–1.9 fold for all cultures, whereas enhanced quantity of stearic acid (C18:0) (~2 fold) was observed only in 5 ppm Cd cultures (Fig. 5D). These results are in line with the earlier report on *Monoraphidium* sp. QLY-1, where Cd stress led to significant increase in palmitic acid (Zhao et al., 2019). Among the unsaturated fatty acids (C18:1, C18:2), relative quantities of oleic acid (C18:1) and linoleic acid (C18:2) reduced by ~ 1.3–1.5 fold in Cd spiked cells. Interestingly cultures cultivated at 10 ppm and 25 ppm Cd augmented ~4% palmitoleic acid (C16:1). In addition to palmitoleic acid, presence of ~5% hexadecatrienoic acid (C16:3) was observed in 25 ppm Cd cells which highlights the role of PUFA in combating the oxidative stress (Fig. 5D). A complete absence of myristic acid (C14:0) and hexadecadienoic acid methyl ester (C16:2) was recorded in all Cd spiked cultures. The overall changes in fatty acid components resulted in significant decline in UFA/SFA ratio from 2.26 in control to 1.03, 1.32, and 1.13 in 5, 10, and 25 ppm Cd spiked, respectively. Such change in UFA/SFA ratio clearly indicates the extent of Cd toxicity in the cells, and the adaptive modulations accompanied by the cells to maintain the fluidity of their cell membrane.

In order to evaluate the applicability of derived lipid for utilization as biodiesel, physical properties based on empirical formula were calculated and has been presented in Table 1. Saponification value (SV) gives a direct measure of ester linkage present in the sample. The high SV (>240 mg KOH) shows the applicability of the oil more as soap rather than biodiesel. The SV obtained for Cd spiked cultures falls in the range of 130–150 mg/KOH which lie under the acceptable limit (220–240 mg KOH). Further, the estimation of iodine values (IV) obtained for Cd spiked cells were between 32 and 53 g I_2/100 g indicated that oil produced under Cd stress has low tendency to form gum. Cetane number (CN) represents the combustion and ignition properties of the derived fuel (Francisco et al., 2010). The CN values in Cd spiked cells were decreased in comparison to control (78), but were still higher than the prescribed minimum limit of 47, which ensures lower NOx emission.

Long chain saturation factor (LCSF) represents the portion of saturated fatty acids in the oil and is useful to estimate the applicability of the derived oil in cold countries in terms of cold filter plugging point (CFFP). CFPP is the transition temperature where oil gets converted to solid and is significant in determining the feasibility of the oil. The derived biodiesel in this study has CFFP value in the range of −1 to −5 °C, suggesting its acceptable performance at lower temperatures. Oxidative stability (OS) and higher heating value (HHV) are other crucial parameters that address the degradation propensity and energy potential of the derived fuel (Pullen and Saeed, 2014). In this study, oxidative stability of 25–19 h with a higher heating value of 43–44 MJ/kg in Cd spiked cells, ensure long storage and high energy potential of the derived fuel. Kinematic viscosity (KV) is an important fuel property that signifies the adequate supply of fuel to the combustion chamber in terms of its flow and speed. The values of KV obtained for all the cultures fall within the range of 1.9–6.0 mm^2/s and ensured appropriate fuel supply to engine (Ramírez-Verduzco et al., 2012). All the estimated biodiesel properties in this study abided the American and European standards and suggest that biodiesel derived from *Scenedesmus* sp. IITRIND2 during Cd mitigation is of vehicular quality.

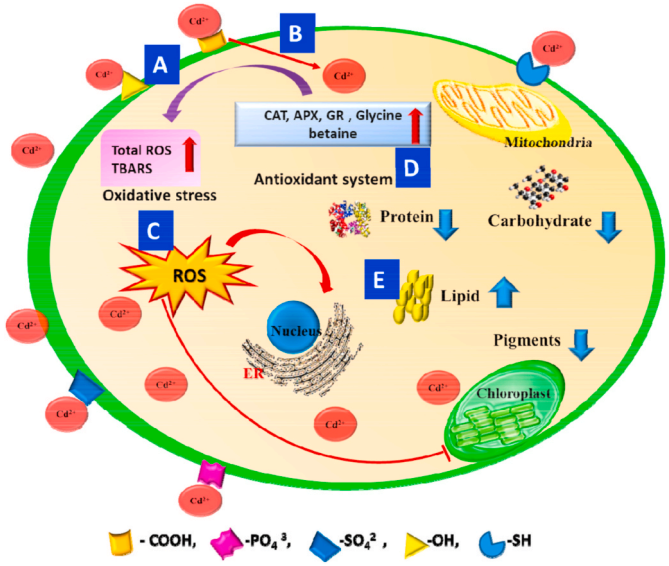

Fig. 6. Schematic representation illustrating the tolerance mechanism adopted by *Scenedesmus* sp. IITRIND2 to survive in the toxic concentrations of cadmium. Various steps involved in the bioremediation of Cd by *Scenedesmus* sp. IITRIND2 involves: (A) Interaction of Cd ions with functional groups present on the cell surface; (B) bioaccumulation of Cd ions inside the cell; (C) ROS generation/ oxidative stress causing lipid peroxidation and inhibiting biosynthesis of photosynthetic pigments; (D) activation of antioxidant machinery comprising enzymes and osmolytes and; (E) alteration in biochemical components thus resulting in enhanced lipid production.

4. Conclusions

The current study demonstrated the dynamic and temporal behavior of *Scenedesmus* sp. IITRIND2 to adapt itself under high concentrations of Cd (5–25 ppm). The microalga exhibited a high IC_{50} value of 31.7 ppm, and effectively removed ~80–90% Cd from the media. The Cd ions attached with the functional groups on the cells surface eventually get internalized and generate excessive ROS causing increased lipid peroxidation (TBARS) and inhibited synthesis of pigments. The oxidative stress due to ROS was scavenged by the enzymatic (CAT, GR, and APX) and non-enzymatic (glycine-betaine) antioxidant molecules. Further, the microalgae cells accustomed their carbon pools towards lipid biosynthesis on expenditure of carbohydrate and protein pools to reinstate cellular redox balance aiding their survival under Cd stress. The schematic representing the underlying mechanism adopted by *Scenedesmus* sp. IITRIND2 against Cd toxicity has been depicted in Fig. 6. In a nut-shell, the current study highlights an integrative approach combining phycoremediation of Cd ions along with lipid production as a sustainable concept of biorefinery. Moreover, the fatty acid composition and physical properties of the derived biodiesel following the American and European standards evidenced the applicability of *Scenedesmus* sp. IITRIND2 for cost-effective and eco-friendly biodiesel production. Further studies involving integrated omics approaches are essential to shed light on the details of interconnected molecular pathways involved in the adaptive response to Cd.

Declaration of competing interest

The authors declare that they have no known competing financial interests or personal relationships that could have appeared to influence the work reported in this paper.

Acknowledgements

ST acknowledge the MHRD fellowship from IIT-Roorkee for pursuing Ph.D. KMP acknowledge the support of Grants GKC-01/2016–17/212/ NMCG-Research from NMCG-MoWR, CRG/2018/001329 from SERB-DST, and DBT-IYBA fellowship, Govt. of India. The authors sincerely thank the analytical and microscopic facilities at Institute Instrumentation Centre at IIT-Roorkee.

Appendix A. Supplementary data

Supplementary data to this article can be found online at https://doi.org/10.1016/j.chemosphere.2021.131196.

Credit author statement

Shweta Tripathi: Conceptualization, Methodology, Experiments, Data Formal analysis, Writing – original draft, Neha Arora: Methodology, Data Formal analysis, Writing – review & editing, Vikas Pruthi: Supervision, Writing – review & editing, Krishna Mohan Poluri: Conceptualization, Supervision, Writing – review & editing, Funding acquisition

References

Afkar, E., Ababna, H., Fathi, A.A., 2010. Toxicological response of the green alga Chlorella vulgaris, to some heavy metals. Am. J. Environ. Sci. 6, 230–237. https://doi.org/10.3844/ajessp.2010.230.237.

Ajayan, K.V., Harilal, C.C., Selvaraju, M., 2018. Phycoremediation resultant lipid production and antioxidant changes in green microalgae Chlorella. Int. J. Phytoremediation 20, 1144–1151. https://doi.org/10.1080/15226514.2017.1413333.

Arora, N., Patel, A., Sartaj, K., Pruthi, P.A., Pruthi, V., 2016. Bioremediation of domestic and industrial wastewaters integrated with enhanced biodiesel production using novel oleaginous microalgae. Environ. Sci. Pollut. Res. 23, 20997–21007. https://doi.org/10.1007/s11356-016-7320-y.

Arora, N., Gulati, K., Patel, A., Pruthi, P.A., Mohan, K., Pruthi, V., 2017a. A hybrid approach integrating arsenic detoxi fi cation with biodiesel production using oleaginous microalgae. Algal Res 24, 29–39. https://doi.org/10.1016/j.algal.2017.03.012.

Arora, N., Patel, A., Sharma, M., Mehtani, J., Pruthi, P.A., Pruthi, V., Poluri, K.M., 2017b. Insights into the enhanced lipid production characteristics of a fresh water microalga under high salinity conditions. Ind. Eng. Chem. Res. 56, 7413–7421. https://doi.org/10.1021/acs.iecr.7b00841.

Arora, N., Dubey, D., Sharma, M., Patel, A., Guleria, A., Pruthi, P.A., 2018. NMR-based metabolomic approach to elucidate the differential cellular NMR-based metabolomic approach to elucidate the di ff erential cellular responses during mitigation of arsenic (III , V) in a green microalga. ACS Omega 3, 11847–11856. https://doi.org/10.1021/acsomega.8b01692.

Arora, N., Kumari, P., Kumar, A., Gangwar, R., Gulati, K., Pruthi, P.A., Prasad, R., Kumar, D., Pruthi, V., Poluri, K.M., 2019. Biotechnology for Biofuels Delineating the Molecular Responses of a Halotolerant Microalga Using Integrated Omics Approach to Identify Genetic Engineering Targets for Enhanced TAG Production. https://doi.org/10.1186/s13068-018-1343-1.

Arunakumara, K.K.I.U., Zhang, X., 2007. Heavy metal bioaccumulation and toxicity with special reference to microalgae. J. Ocean Univ. China 7, 60–64. https://doi.org/10.1007/s11802-008-0060-y.

Balzano, S., Sardo, A., Blasio, M., Chahine, T.B., Dell'Anno, F., Sansone, C., Brunet, C., 2020. Microalgal metallothioneins and phytochelatins and their potential use in bioremediation. Front. Microbiol. 11, 1–16. https://doi.org/10.3389/fmicb.2020.00517.

Bates, L.S., Waldren, R.P., Teare, I.D., 1973. Rapid determination of free proline for water-stress studies. Plant Soil 39, 205–207.

Belghith, T., Athmouni, K., Bellassoued, K., 2016. Physiological and Biochemical Response of Dunaliella Salina to Cadmium Pollution 991–999. https://doi.org/10.1007/s10811-015-0630-5.

Bligh, E.G., Dyer, W.J., 1959. Canadian journal of biochemistry and physiology. Can. J. Biochem. Physiol. 37, 911–917.

Cheng, J., Qiu, H., Chang, Z., Jiang, Z., Yin, W., 2016. The effect of cadmium on the growth and antioxidant response for freshwater algae Chlorella vulgaris. SpringerPlus 5, 1–8. https://doi.org/10.1186/s40064-016-2963-1.

da Silva Ferreira, V., Sant'Anna, C., 2017. Impact of culture conditions on the chlorophyll content of microalgae for biotechnological applications. World J. Microbiol. Biotechnol. 33, 1–8.

Dean, A.P., Hartley, A., Mcintosh, O.A., Smith, A., Feord, H.K., Holmberg, N.H., King, T., Yardley, E., White, K.N., Pittman, J.K., 2019. Science of the Total Environment Metabolic adaptation of a Chlamydomonas acidophila strain isolated from acid mine drainage ponds with low eukaryotic diversity. Sci. Total Environ. 647, 75–87. https://doi.org/10.1016/j.scitotenv.2018.07.445.

Dhir, B., Sharmila, P., Saradhi, P.P., 2004. Hydrophytes lack potential to exhibit cadmium stress induced enhancement in lipid peroxidation and accumulation of

proline. Aquat. Toxicol. 66, 141–147. https://doi.org/10.1016/j.aquatox.2003.08.005.
Doshi, H., Ray, A., Kothari, I.L., 2007. Bioremediation potential of live and dead Spirulina: spectroscopic, kinetics and SEM studies. Biotechnol. Bioeng. 96, 1051–1063.
D'Souza, L., Devi, P., Divya Shridhar, M.P., Naik, C.G., 2008. Use of fourier transform infrared (FTIR) spectroscopy to study. Cadmium-Induced Changes in Padina 91, 135–143.
Duque, D., Montoya, C., Botero, L.R., 2019. Cadmium (Cd) tolerance evaluation of three strains of microalgae of the genus Ankistrodesmus, C hlorella and Scenedesmus. Rev. Fac. Ing. Univ. Antioquia 88–95.
Francisco, É.C., Neves, D.B., Jacob-Lopes, E., Franco, T.T., 2010. Microalgae as feedstock for biodiesel production: carbon dioxide sequestration, lipid production and biofuel quality. J. Chem. Technol. Biotechnol. 85, 395–403. https://doi.org/10.1002/jctb.2338.
Ganapathy, T., Murugesan, K., Gakkhar, R.P., 2009. Performance optimization of Jatropha biodiesel engine model using Taguchi approach. Appl. Energy 86, 2476–2486. https://doi.org/10.1016/j.apenergy.2009.02.008.
Gimmler, H., Treffny, B., Kowalski, M., Zimmermann, U., 1991. The resistance of Dunaliella acidophila against heavy metals: the importance of the zeta potential. J. Plant Physiol. 138, 708–716.
Hasanuzzaman, M., Bhuyan, M.H.M., Anee, T.I., Parvin, K., Nahar, K., Mahmud, J. Al, Fujita, M., 2019. Regulation of ascorbate-glutathione pathway in mitigating oxidative damage in plants under abiotic stress. Antioxidants 8, 384.
Hossain, M.A., Piyatida, P., da Silva, J.A.T., Fujita, M., 2012. Molecular mechanism of heavy metal toxicity and tolerance in plants: central role of glutathione in detoxification of reactive oxygen species and methylglyoxal and in heavy metal chelation. J. Bot., Le 1–37. https://doi.org/10.1155/2012/872875, 2012.
Hossain, M.A., Burritt, D.J., Fujita, M., 2015. Proline and glycine betaine modulate cadmium-induced oxidative stress tolerance in plants. Plant-Environment Interact. 97–123. https://doi.org/10.1002/9781119081005.ch6.
Järup, L., Åkesson, A., 2009. Current status of cadmium as an environmental health problem. Toxicol. Appl. Pharmacol. 238, 201–208.
John, R., Ahmad, P., Gadgil, K., Sharma, S., 2008. Effect of cadmium and lead on growth, biochemical parameters and uptake in Lemna polyrrhiza L. Plant Soil Environ. 54, 262.
Kanamarlapudi, S., Chintalpudi, V.K., Muddada, S., 2018. Application of biosorption for removal of heavy metals from wastewater. Biosorption 18, 69.
Kinuthia, G.K., Ngure, V., Beti, D., Lugalia, R., Wangila, A., Kamau, L., 2020. Levels of heavy metals in wastewater and soil samples from open drainage channels in Nairobi, Kenya: community health implication. Sci. Rep. 10, 1–13. https://doi.org/10.1038/s41598-020-65359-5.
Knothe, G., 2006. Analyzing biodiesel: standarts and other methods. JAOCS (J. Am. Oil Chem. Soc.) 83. https://doi.org/10.1007/s11746-006-5033-y.
Kováčik, J., Babula, P., Peterková, V., Hedbavny, J., 2017. Long-term impact of cadmium shows little damage in Scenedesmus acutiformis cultures. Algal Res 25, 184–190. https://doi.org/10.1016/j.algal.2017.04.029.
Laurens, L.M.L., Van Wychen, S., McAllister, J.P., Arrowsmith, S., Dempster, T.A., McGowen, J., Pienkos, P.T., 2014. Strain, biochemistry, and cultivation-dependent measurement variability of algal biomass composition. Anal. Biochem. 452, 86–95. https://doi.org/10.1016/j.ab.2014.02.009.
Li, B., Pan, D., Zheng, J., Cheng, Y., Ma, X., Huang, F., Lin, Z., 2008. Microscopic investigations of the Cr (VI) uptake mechanism of living Ochrobactrum anthropi. Langmuir 24, 9630–9635.
Liang, X., Zhang, L., Natarajan, S.K., Becker, D.F., 2013. Proline mechanisms of stress survival. Antioxidants Redox Signal. 19, 998–1011.
Lichtenthaler, H.K., 1987. Chlorophylls and carotenoids: pigments of photosynthetic biomembranes. Methods Enzymol. 148, 350–382. https://doi.org/10.1016/0076-6879(87)48036-1.
Lu, J., Ma, Y., Xing, G., Li, W., Kong, X., Li, J., Wang, L., Yuan, H., Yang, J., 2019. Revelation of microalgae ' s lipid production and resistance mechanism to ultra-high Cd stress by integrated transcriptome and physiochemical analyses *. Environ. Pollut. 250, 186–195. https://doi.org/10.1016/j.envpol.2019.04.018.
Lu, M.-M., Gao, F., Li, C., Yang, H.-L., 2021. Response of microalgae Chlorella vulgaris to Cr stress and continuous Cr removal in a membrane photobioreactor. Chemosphere 262, 128422.
McElroy, J.A., Hunter, M.I., 2019. Cadmium: a new risk factor for endometrial cancer?.
Mehta, S., Gaur, J., 1999. Heavy-metal-induced proline accumulation and its role in ameliorating metal toxicitiy in Chlorella vulgaris. New Phytol. 143, 253–259.
Monteiro, C.M., Castro, P.M.L., Malcata, F.X., Instituto, I., Carlos, A., Campos, O., Maia, C., Pedro, P.–A.S., 2012. Metal Uptake by Microalgae : Underlying Mechanisms and Practical Applications. https://doi.org/10.1002/btpr.1504.
Napan, K., Teng, L., Quinn, J.C., Wood, B.D., 2015. Impact of heavy metals from flue gas integration with microalgae production. Algal Res 8, 83–88. https://doi.org/10.1016/j.algal.2015.01.003.
Perales-Vela, H.V., Peña-Castro, J.M., Cañizares-Villanueva, R.O., 2006. Heavy metal detoxification in eukaryotic microalgae. Chemosphere 64, 1–10. https://doi.org/10.1016/j.chemosphere.2005.11.024.
Pérez-Rama, M., Alonso, J.A., López, C.H., Vaamonde, E.T., 2002. Cadmium removal by living cells of the marine microalga Tetraselmis suecica. Bioresour. Technol. 84, 265–270.
Pfeiffer, T., Camagajevac, I., Maronic, D., Maksimovic, I., 2018. Regulation of photosynthesis in algae under metal stress. Environ. Photosynth. A Futur. Prospect.
Piotrowska-Niczyporuk, A., Bajguz, A., Zambrzycka, E., Godlewska-zyłkiewicz, B., 2012. Phytohormones as regulators of heavy metal biosorption and toxicity in green alga Chlorella vulgaris (Chlorophyceae). Plant Physiol. Biochem. 52, 52–65. https://doi.org/10.1016/j.plaphy.2011.11.009.
P S, C., Sanyal, D., Dasgupta, S., Banik, A., 2020. Cadmium biosorption and biomass production by two freshwater microalgae Scenedesmus acutus and Chlorella pyrenoidosa: an integrated approach. Chemosphere. https://doi.org/10.1016/j.chemosphere.2020.128755, 128755.
Pullen, J., Saeed, K., 2014. Experimental study of the factors affecting the oxidation stability of biodiesel FAME fuels. Fuel Process. Technol. 125, 223–235. https://doi.org/10.1016/j.fuproc.2014.03.032.
Ramírez-Verduzco, L.F., Rodríguez-Rodríguez, J.E., Jaramillo-Jacob, A.D.R., 2012. Predicting cetane number, kinematic viscosity, density and higher heating value of biodiesel from its fatty acid methyl ester composition. Fuel 91, 102–111. https://doi.org/10.1016/j.fuel.2011.06.070.
Ramos, M.J., Fernández, C.M., Casas, A., Rodríguez, L., Pérez, Á., 2009. Influence of fatty acid composition of raw materials on biodiesel properties. Bioresour. Technol. 100, 261–268. https://doi.org/10.1016/j.biortech.2008.06.039.
Samadani, M., Perreault, F., Oukarroum, A., Dewez, D., 2018. Effect of cadmium accumulation on green algae Chlamydomonas reinhardtii and acid-tolerant Chlamydomonas CPCC 121. Chemosphere 191, 174–182.
Satarug, S., Baker, J.R., Urbenjapol, S., Haswell-elkins, M., Reilly, P.E.B., Williams, J., Moore, R., 2003. A global perspecti v e on cadmium pollution and toxicity in non-occupationally exposed population 137.
Schaedle, M., Bassham, J.A., 1977. Chloroplast Glutathione Reductase1, pp. 1011–1012.
Shaikh, K.M., Nesamma, A.A., Abdin, M.Z., Jutur, P.P., 2019. Molecular profiling of an oleaginous trebouxiophycean alga Parachlorella kessleri subjected to nutrient deprivation for enhanced biofuel production. Biotechnol. Biofuels 12, 1–15. https://doi.org/10.1186/s13068-019-1521-9.
Shanmugam, G., Polavarapu, P.L., Láng, E., Majer, Z., 2012. Conformational analysis of amyloid precursor protein fragment containing amino acids 667-676, and the effect of d-Asp and iso-Asp substitution at Asp 672 residue. J. Struct. Biol. 177, 621–629. https://doi.org/10.1016/j.jsb.2012.01.012.
Sharma, S.S., Dietz, K.J., 2006. The significance of amino acids and amino acid-derived molecules in plant responses and adaptation to heavy metal stress. J. Exp. Bot. 57, 711–726. https://doi.org/10.1093/jxb/erj073.
Sharma, K.K., Schuhmann, H., Schenk, P.M., 2012. High lipid induction in microalgae for biodiesel production. Energies 5, 1532–1553. https://doi.org/10.3390/en5051532.
Shivaji, S., Dro, S.V.L., 2019. Scenedesnus rotundus isolated from the petroleum effluent employs alternate mechanisms of tolerance to elevated levels of Cadmium and Zinc. https://doi.org/10.1038/s41598-019-44374-1, 1-15.
Stiborová, M., Ditrichová, M., BŘEzinová, A., 1987. Effect of heavy metal ions on growth and biochemical characteristics of photosynthesis of barley and maize seedlings. Biol. Plant. (Prague) 29, 453.
Sytar, O., Kumar, A., Latowski, D., Kuczynska, P., Strzałka, K., Prasad, M.N.V., 2013. Heavy metal-induced oxidative damage, defense reactions, and detoxification mechanisms in plants. Acta Physiol. Plant. 35, 985–999. https://doi.org/10.1007/s11738-012-1169-6.
Tripathi, S., Poluri, K.M., 2021a. Adaptive and tolerance mechanism of microalgae in removal of cadmium from wastewater. In: Algae. Springer, pp. 63–88.
Tripathi, S., Poluri, K.M., 2021b. Metallothionein-and phytochelatin-assisted mechanism of heavy metal detoxification in microalgae. Approaches to Remediat. Inorg. Pollut. 323.
Tripathi, S., Arora, N., Gupta, P., Pruthi, P.A., Poluri, K.M., Pruthi, V., 2019. Microalgae: an emerging source for mitigation of heavy metals and their potential implications for biodiesel production. In: Advanced Biofuels. Elsevier, pp. 97–128.
Valadez-bustos, M.G., Aguado-santacruz, G.A., Tiessen-favier, A., Robledo-paz, A., Mu, A., Santacruz-varela, A., Rasc, Q., 2016. A Reliable Method for Spectrophotometric Determination of glycine Betaine in Cell Suspension and Other Systems, vol. 498, pp. 47–52. https://doi.org/10.1016/j.ab.2015.12.015.
Vitova, M., Bisova, K., Kawano, S., Zachleder, V., 2014. Accumulation of energy reserves in algae: from cell cycles to biotechnological applications. Biotechnol. Adv. 33, 1204–1218. https://doi.org/10.1016/j.biotechadv.2015.04.012.
Yang, J.S., Cao, J., Xing, G.L., Yuan, H.L., 2015. Lipid production combined with biosorption and bioaccumulation of cadmium, copper, manganese and zinc by oleaginous microalgae Chlorella minutissima UTEX2341. Bioresour. Technol. 175, 537–544. https://doi.org/10.1016/j.biortech.2014.10.124.
Yilancioglu, K., Cokol, M., Pastirmaci, I., Erman, B., Cetiner, S., 2014. Oxidative stress is a mediator for increased lipid accumulation in a newly isolated Dunaliella salina strain. PloS One 9, e91957. https://doi.org/10.1371/journal.pone.0091957.
Zhang, Y.M., Chen, H., He, C.L., Wang, Q., 2013. Nitrogen starvation induced oxidative stress in an oil-producing green alga Chlorella sorokiniana C3. PloS One 8, 1–12. https://doi.org/10.1371/journal.pone.0069225.
Zhao, Y., Song, X., Yu, L., Han, B., Li, T., Yu, X., 2019. In fl uence of cadmium stress on the lipid production and cadmium bioresorption by Monoraphidium sp . QLY-1. Energy Convers. Manag. 188, 76–85. https://doi.org/10.1016/j.enconman.2019.03.041.
Zhu, Y.L., Zayed, A.M., Qian, J.H., de Souza, M., Terry, N., 1999. Phytoaccumulation of trace elements by wetland plants: II. Water hyacinth. J. Environ. Qual. 28, 339–344. https://doi.org/10.2134/jeq1999.00472425002800010042x.
Zhu, Q., Guo, S., Wen, F., Zhang, X., Wang, C., Si, L., 2019. Transcriptional and physiological responses of Dunaliella salina to cadmium reveals time-dependent turnover of ribosome , photosystem , and ROS- scavenging pathways. Aquat. Toxicol. 207, 153–162. https://doi.org/10.1016/j.aquatox.2018.12.007.
Zwolak, I., 2020. The role of selenium in arsenic and cadmium toxicity: an updated review of scientific literature. Biol. Trace Elem. Res. 193, 44–63. https://doi.org/10.1007/s12011-019-01691-w.